Does lattice vibration drive diffusion in zeolites?

Dmitry I. Kopelevich and Hsueh-Chia Chang
Department of Chemical Engineering, University of Notre Dame, Notre Dame, Indiana 46556

(Received 28 August 2000; accepted 1 December 2000)

A method of estimation of the effect of lattice vibration as a driving force for sorbate diffusion in zeolites is proposed. A realistic lattice model is employed to cut off unrealistic long vibrational modes and eliminate feedback due to lattice periodicity. A generalized Langevin equation for sorbate motion is then derived with the magnitude of the lattice vibration captured by two parameters, μ and ν, which can be readily computed for any system. The effect of lattice vibration is then estimated for a variety of sorbate–zeolite pairs. Lattice vibration is found to be a negligible driving force for some systems (e.g., methane and xenon in silicalite) and an important driving force for other systems. In the latter case, the lattice vibration can provide either linear stochastic Langevin-type force (e.g., for benzene in silicalite) or nonlinear deterministic force (e.g., for argon in sodalite). © *2001 American Institute of Physics.* [DOI: 10.1063/1.1343072]

I. INTRODUCTION

Understanding molecular transport inside zeolite pores is important for optimal designs of zeolites as sieves, sorbents, and catalysts. Diffusion in zeolites has peculiar dependence on temperature, loading, and molecular structure which does not appear in more conventional nonequilibrium bulk gas diffusion and Knudsen diffusion due to collisions. Such differences are due to the lattice medium around the sorbate molecule, which is periodic over a large scale but not so locally, and the peculiar interaction between the two. In contrast to discrete bombardment by a homogeneously distributed medium in gas diffusion, the sorbate molecule in a zeolite is under constant influence of its highly anisotropic local lattice medium. Other than the static lattice–sorbate interaction that defines the potential landscape the sorbate must traverse, there must be either a deterministic or stochastic driving force to drive a single sorbate molecule over the landscape in the dilute limit.

For very large molecules like long-chain hydrocarbons, the deterministic dynamics of the numerous fast (compared to the diffusion time) intramolecular vibration and torsion modes can drive the center- of-mass of the molecule.[1] For small sorbates, however, the small number of fast modes implies that they are not significant as a deterministic driving force. However, even inert gas atoms are observed to undergo diffusive transport through zeolites at the infinite dilution limit.[2] It is then often assumed that such transport of small sorbates is driven by stochastic vibration of the zeolite lattice which now acts as a thermal bath.[3,4] This stochastic force is then analogous to that provided by molecule collision for bulk gas diffusion and by diffuse reflection by wall for Knudsen diffusion in larger pores. For zeolite diffusion, the sorbate would hence feel the fluctuating and static components of the lattice–sorbate potential everywhere in the space. In fact, lattice vibration is always used as an explanation why sorbates can sometimes penetrate pores of comparable size or even smaller. Such lattice vibration of small pores must also be important for large molecules. Their intramolecular fast modes surely cannot drive the molecule through a rigid pore comparable or smaller than the sorbate's width.

One particular example is argon in sodalite. The zeolite is impenetrable by the sorbate at low temperature and pressure but a finite diffusivity is detected at high temperature and pressure.[5] Since the window diameter ($\sim$2.3 Å) of this zeolite is smaller than the sorbate diameter ($\sim$3.8 Å), the penetration at high temperature must be due to large-amplitude lattice vibration that opens the pore dynamically.

However, the necessity of stochastic noise from lattice vibration to drive diffusive motion in a zeolite is questioned by a sequence of molecular dynamics (MD) simulations carried out for methane diffusion in a silicalite zeolite crystal.[6–8] Most of these MD simulations are conducted with a fixed zeolite lattice and without internal vibration, but Demontis *et al.*[8] simulate the lattice vibration in detail. However, all of them observe diffusive-type behavior with a linearly-growing variance and produce roughly the same diffusivities which are in good agreement with experimental measurements. This suggests that, at least in this sorbate–zeolite system, the sorbate is oblivious to the lattice vibration.

The goal of this study is to estimate the importance of lattice vibration in sorbate diffusion and how the sorbate can, in turn, induce the lattice vibration. We do this by developing a stochastic description for the motion of the sorbate, treating the lattice both as a thermal bath and as an active participant of deterministic dynamics with the sorbate. A lattice thermal bath model was developed by Zwanzig[3] and Tsekov and Ruckenstein.[4] These authors assumed a harmonic lattice and linear coupling between lattice vibration and sorbate. This allowed them to derive a generalized Langevin equation, i.e., a stochastic equation with a non-Markovian noise source. Then under the assumption of a Debye distribution of lattice frequencies, the noise can be reduced to a Markovian one due to a specific frequency dependence of the lattice–sorbate coupling. This Debye assumption essentially neglects high-frequency optical vibration modes and stipulates that the dominant ones are the

low-frequency acoustic modes. This does not seem to have any physical sense since the acoustic modes correspond to long sound waves in a crystal and they cannot be excited by the motion of a single sorbate molecule, nor can they make an important contribution as a driving force for diffusion across several unit cells whose combined length ($\sim$10 to 100 Å) is much shorter than the wavelength of macroscopic acoustic modes. Such coupling may be possible if acoustic modes are sustained artificially for long durations at large amplitudes but highly unlikely under the usual circumstances. This is especially true when nonlinear vibration is allowed, as it should be at the large amplitudes of the Debye approximation. Nonlinearity tends to focus the lattice vibration into localized wave packets.[9] These wave packets would then pass by the sorbate rapidly, further minimizing the possibility of interaction between the two.

To exacerbate the problem, classical lattice models are often assumed to be periodic. This introduces artificial feedback in MD simulations through the periodic boundary conditions. Lattice vibration triggered by the sorbate could return and drive the sorbate. In fact, this unrealistic feedback, when simulated on the computer, can resonantly excite the long acoustic waves and sustain them indefinitely to produce artificial interaction with the sorbate. There would then be highly exaggerated sorbate transport rate that is not observed in reality. Both the periodic feedback and the coupling with the long acoustic waves must hence be cut off with a new model.

In our model, we introduce this cut off by allowing only a finite subset of lattice atoms L_S near the sorbate to interact with the sorbate. The remaining lattice atoms L_F outside L_S are assumed to be in thermal equilibrium. Moreover, deterministic dynamic energy transfer is only from L_S to L_F while the opposite transfer is in the form of thermal equilibration (thermostating) only. This removes feedback due to periodicity and, in case of nonlinear vibration, allows excited localized lattice wave packets (held together by nonlinearity) to radiate away from the sorbate.

The size of L_S then represents the cut off length scale for excitable acoustic modes and sorbate–lattice interaction. Since it is unknown, we vary L_S and examine its effect on the sorbate transport rate. The latter quantity is observed to reach an asymptote when the L_S radius exceeds $\sim$9 Å, indicating that the sorbate can only interact with lattice atoms within this radius. Even if the radius of L_S is at the computational maximum (13 Å), the effect on the sorbate is still significantly less than the periodic lattice model with large wavelength. The periodic model is hence deficient even when large periodicity is assumed. Physically, acoustic waves propagate much faster than sorbate motion and a standing acoustic wave allowed by the periodic lattice is impossible in a large zeolite medium whose acoustic modes are allowed to propagate away from the sorbate.

A generalized Langevin equation for the sorbate is derived with our model and used to estimate the contribution of lattice vibration to sorbate transport. Parameters μ and ν are introduced to quantify its importance.

In this work we consider xenon, methane, ethane, and benzene sorbates in zeolites sodalite (SOD), silicalite (MFI), and mordenite (MOR).[10] The crystal structures of these zeolites are shown in Fig. 1 and are typical of most other zeolites. Sodalite unit cell is a truncated cuboctahedral cage of diameter 6.6 Å. These cages are connected by windows, which are formed by six rings of oxygen atoms and have diameter 2.3 Å. Even though these windows are too narrow for most sorbates to pass, it is worthwhile to study behavior of sorbates inside a sodalite cage due to important applications in storage of gases.[5] Mordenite crystal consists of parallel one-dimensional twelve-ring channels with small eight-ring side pockets bordering the channels. The main channels have an elliptical cross section with principal axes 6.5 and 7.0 Å. Silicalite contains a network of two intersecting channels — straight and zigzag ones. These channels are formed by ten rings and thus have an intermediate size between sodalite and mordenite pores. The straight channels run in the *y*-direction and have elliptical cross section of size 5.7–5.8 $\times$5.1–5.2 Å and the zigzag channels run in the *x*-direction and have a nearly circular cross section of diameter 5.4 Å.

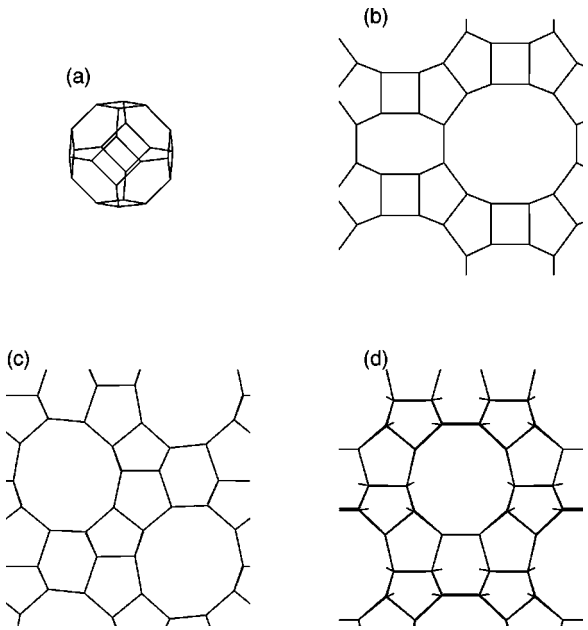

FIG. 1. Crystal structures of considered zeolites (only Si atoms are shown): (a) sodalite, (b) mordenite (view along the channel, one of the eight-ring side pockets is also shown), (c) silicalite (view along straight channels), (d) silicalite (view along zigzag channels).

It is found that although stochastic lattice vibration provides a driving force for sorbate diffusion in some zeolite–sorbate pairs (e.g., for benzene in silicalite), it is unimportant in other systems (e.g., for methane or xenon in silicalite). Sorbate transport in the latter systems must then be driven by other deterministic or stochastic forces on the sorbate molecule in a rigid zeolite, as is consistent with earlier simulations for these systems.[6–8] Without the stochastic forcing and dissipation through coupling with thermal lattice vibration, the usual fluctuation–dissipation theorem for bulk transport driven by thermal fluctuation is also not applicable and sorbate transport in zeolite must then be due to a non-Langevin driving force.

One possibility is a deterministic force due to KAM chaos which was suggested in our earlier article[11] on diffu-

sion of spherical molecules through single-pore zeolites. When the momentum of the sorbate along the transport axis is transferred to the transverse degrees of freedom due to asymmetric geometry of the pore, this produces a deterministic chaotic driving force and the resulting transport is shown to be diffusive with a diffusivity close to the observed one. Similar diffusion mechanism was conjectured for surface diffusion of a hydrogen adatom.[12] In this case, the driving force is due to coupling between horizontal and vertical degrees of freedom of the adatom.

In terms of MD simulation efforts, our current result allows us to explicitly determine whether one has to simulate the lattice vibration in detail or not — extremely useful information.

II. STOCHASTIC DESCRIPTION

In this section, we present our model for the sorbate–zeolite system and derive the generalized Langevin equation for the sorbate transport. We consider first the motion of a sorbate molecule with N degrees of freedom inside a zeolite pore in the classical mechanics approximation. The configuration of the molecule and its position in space are completely specified by N generalized coordinates q_i, $i=1,\ldots,N$, and the position of an sth atom of the molecule is given by $\mathbf{X}_s=\mathbf{X}_s(\mathbf{q})$.

Kinetic energy of the sorbate is

$$T=\frac{1}{2}\sum_s M_s\dot{\mathbf{X}}_s^2=\frac{1}{2}\dot{\mathbf{q}}\mathbf{A}(\mathbf{q})\dot{\mathbf{q}}, \tag{1}$$

where

$$A_{ij}(\mathbf{q})=\sum_s M_s\frac{\partial\mathbf{X}_s}{\partial q_i}\cdot\frac{\partial\mathbf{X}_s}{\partial q_j}, \tag{2}$$

and M_s is mass of the sth atom in the molecule. Generalized momentum of the sorbate is $\mathbf{p}=\partial T/\partial\dot{\mathbf{q}}=\mathbf{A}(\mathbf{q})\dot{\mathbf{q}}$ and hence the Hamiltonian of a free sorbate is

$$H_S=\tfrac{1}{2}\mathbf{p}\mathbf{A}^{-1}(\mathbf{q})\mathbf{p}+U(\mathbf{q}), \tag{3}$$

where $U(\mathbf{q})$ is the intramolecular potential energy. We neglect fast intramolecular vibration such as bond length stretching and bond angle bending, thus retaining only slow intramolecular motions such as torsional motion.

In particular, for a point–mass approximation, the generalized coordinates $\mathbf{q}$ of the sorbate molecule coincide with the coordinates $\mathbf{X}$ of the center-of-mass of the molecule, intramolecular potential energy U vanishes, and the momentum of the molecule is $\mathbf{p}=M\dot{\mathbf{X}}$ where M is the mass of the molecule. Hence, in this case Eq. (3) reduces to

$$H_S=\frac{p^2}{2M}. \tag{4}$$

Consider now motion of a free zeolite lattice. We consider a zeolite crystal of an infinite size. The position of a unit cell in the crystal is given by

$$\mathbf{r}(\mathbf{l})=l_1\mathbf{a_1}+l_2\mathbf{a_2}+l_3\mathbf{a_3},\ l_1,l_2,l_3=0,\pm1,\pm2\ldots, \tag{5}$$

where $\mathbf{a_1}$, $\mathbf{a_2}$, and $\mathbf{a_3}$ are basis vectors of the lattice. There are n atoms in a unit cell and a position of a κth atom is specified by $\mathbf{r}(\kappa)$, $\kappa=1,\ldots,n$. Therefore, position of any atom in the crystal is completely determined by the position of its unit cell $\mathbf{l}$ and its number κ inside the unit cell,

$$\mathbf{r}(\mathbf{l}\kappa)=\mathbf{r}(\mathbf{l})+\mathbf{r}(\kappa). \tag{6}$$

Denote the αth component ($\alpha=1,2,3$) of displacement of the $(\mathbf{l}\kappa)$th atom from its equilibrium position by $\rho_\alpha(\mathbf{l}\kappa)$. The energy of vibrating lattice in the harmonic approximation for the lattice potential energy V is given by

$$H_L=\frac{1}{2}\sum_{\mathbf{l}}\sum_{\kappa=1}^{n} m_\kappa\dot{\mathbf{r}}^2(\mathbf{l}\kappa)+\frac{1}{2}\sum_{\mathbf{l},\mathbf{l}'}\sum_{\kappa,\kappa'=1}^{n}\sum_{\alpha,\beta=1}^{3} V_{\alpha\beta}(\mathbf{l}\kappa,\mathbf{l}'\kappa')\rho_\alpha(\mathbf{l}\kappa)\rho_\beta(\mathbf{l}'\kappa'). \tag{7}$$

Here m_κ is mass of the κth atom of a unit cell and

$$V_{\alpha\beta}(\mathbf{l}\kappa,\mathbf{l}'\kappa')=\left(\frac{\partial^2 V}{\partial r_\alpha(\mathbf{l}\kappa)\partial r_\beta(\mathbf{l}'\kappa')}\right)_0,\quad \alpha,\beta=1,2,3. \tag{8}$$

Here and below the zero subscript indicates that a derivative is calculated at the equilibrium configuration of the crystal lattice. The first derivative of the potential energy of the crystal in the equilibrium configuration vanishes, since the force acting on any particle of the crystal is zero in the equilibrium configuration.

It is convenient to introduce normalized displacements of the atoms from their equilibrium positions,

$$u_\alpha(\mathbf{l}\kappa)=m_\kappa^{1/2}\rho_\alpha(\mathbf{l}\kappa), \tag{9}$$

and thus obtain the following expression for the Hamiltonian of the free lattice:

$$H_L=\frac{1}{2}\sum_{\mathbf{l}\kappa}\sum_{\alpha=1}^{3}\dot{u}_\alpha^2(\mathbf{l}\kappa)+\frac{1}{2}\sum_{\mathbf{l}\kappa}\sum_{\mathbf{l}'\kappa'}\sum_{\alpha,\beta=1}^{3} D_{\alpha\beta}(\mathbf{l}\kappa,\mathbf{l}'\kappa')\times u_\alpha(\mathbf{l}\kappa)u_\beta(\mathbf{l}'\kappa'), \tag{10}$$

where

$$D_{\alpha\beta}(\mathbf{l}\kappa,\mathbf{l}'\kappa')=(m_\kappa m_{\kappa'})^{-1/2}V_{\alpha\beta}(\mathbf{l}\kappa,\mathbf{l}'\kappa') \tag{11}$$

is the lattice dynamical matrix that defines all the vibrational modes and frequencies of the lattice.

We assume that interaction between sorbate and lattice is short-range (e.g., Lennard-Jones) and hence only those lattice atoms that are close enough to the sorbate ''feel'' the latter. This allows us to separate the zeolite lattice into two parts, which we call L_S and L_F (see Fig. 2). The nearby atoms in L_S directly interact with the sorbate. The atoms of L_F constitute the rest of the crystal outside L_S and interact with the sorbate only through phonon waves that come from and go to L_S. As a result, the bonds joining L_S and L_F are never stretched by deterministic dynamics and simply fluctuate stochastically — periodicity is not imposed. (Subindices ''S'' and ''F'' stand for ''sorbate'' and ''free'', respectively).

Note that such a separation is possible because a time scale of sorbate motion is much slower than that of the lattice vibration: A typical diffusivity of small spherical sorbates in zeolites such as xenon and methane is $\sim10^{-8}\,\mathrm{m}^2/\mathrm{s}$ and is even smaller for larger molecules, i.e., it takes at least

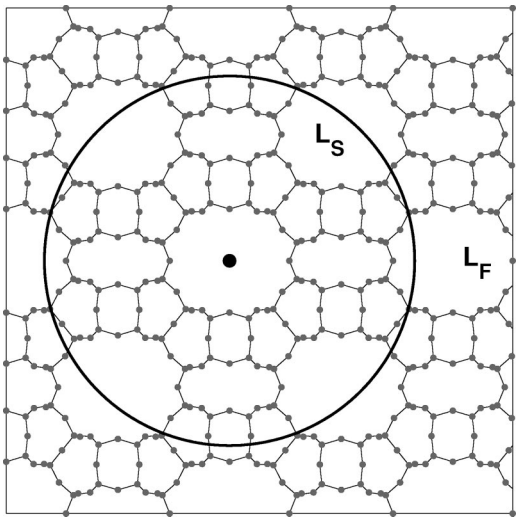

FIG. 2. Definition of L_S and L_F.

10^{-10} s for a sorbate to travel across one crystal unit cell of size ~ 10 Å, whereas frequencies of lattice vibration are in the range $10^{12}-10^{14}\,s^{-1}$. Thus, on the time scale of lattice vibration, our classification of L_S and L_F remains the same. However, such a separation of lattice into two parts would not be possible, for example, in studies of superconductivity, where one has to consider coupling between electron motion and lattice vibration which occur on comparable time scales.

We expand energy Φ of the sorbate–lattice interaction in a power series in the normalized displacements $\mathbf{u}$ of zeolite atoms:

$$\Phi(\mathbf{q},\{\mathbf{r}(\mathbf{l}\kappa)\}) \approx \Phi_0(\mathbf{q}) + \sum_{\mathbf{l}\kappa\in L_S}\sum_{\alpha=1}^{3} f_\alpha(\mathbf{l}\kappa;\mathbf{q})u_\alpha(\mathbf{l}\kappa) + \frac{1}{2}\sum_{\mathbf{l}\kappa\in L_S}\sum_{\mathbf{l}'\kappa'\in L_S}\sum_{\alpha,\beta=1}^{3} G_{\alpha\beta}(\mathbf{l}\kappa,\mathbf{l}'\kappa';\mathbf{q}) \times u_\alpha(\mathbf{l}\kappa)u_\beta(\mathbf{l}'\kappa'), \tag{12}$$

where

$$f_\alpha(\mathbf{l}\kappa;\mathbf{q}) = m_\kappa^{-1/2}\left(\frac{\partial\Phi(\mathbf{q},\{\mathbf{r}(\mathbf{l}\kappa)\})}{\partial r_\alpha(\mathbf{l}\kappa)}\right)_0, \tag{13}$$

$$G_{\alpha\beta}(\mathbf{l}\kappa,\mathbf{l}'\kappa';\mathbf{q}) = (m_\kappa m_{\kappa'})^{-1/2}\left(\frac{\partial^2\Phi(\mathbf{q},\{\mathbf{r}(\mathbf{l}\kappa)\})}{\partial r_\alpha(\mathbf{l}\kappa)\partial r_\beta(\mathbf{l}'\kappa')}\right)_0, \quad \alpha,\beta=1,2,3 \tag{14}$$

represent the additional dynamic force exerted by the $\mathbf{l}\kappa$th lattice atom on the sorbate as the former deviates from its equilibrium position due to vibration.

We further assume that the sorbate–zeolite interaction potential Φ is pairwise additive,

$$\Phi(\mathbf{q},\{\mathbf{r}\}) = \sum_{\mathbf{l}\kappa\in L_S}\sum_{s}^{N}\phi_{s\kappa}(\mathbf{X}_s-\mathbf{r}(\mathbf{l}\kappa)), \tag{15}$$

where $\phi_{s\kappa}$ is the interaction potential between sth atom of the sorbate at position $\mathbf{X}_s$ and κth atom of a zeolite unit cell at $\mathbf{r}(\mathbf{l}\kappa)$. From this pairwise additivity it follows that

$$G_{\alpha\beta}(\mathbf{l}\kappa,\mathbf{l}'\kappa';\mathbf{q}) = \delta_{\mathbf{l},\mathbf{l}'}\delta_{\kappa,\kappa'}G_{\alpha\beta}(\mathbf{l}\kappa,\mathbf{l}\kappa;\mathbf{q}). \tag{16}$$

It is convenient to introduce the following partition of the vector $\mathbf{u}$,

$$\mathbf{u} = \begin{pmatrix}\mathbf{u}^{(S)}\\ \mathbf{u}^{(F)}\end{pmatrix}, \tag{17}$$

where $\mathbf{u}^{(S)}$ [$\mathbf{u}^{(F)}$] is a finite (infinite) vector containing displacements of the L_S (L_F) atoms. Similarly, we partition the dynamical matrix $\mathbf{D}$,

$$\mathbf{D} = \begin{pmatrix}\mathbf{D}^{(S)} & \mathbf{D}^{(SF)}\\ \mathbf{D}^{(FS)} & \mathbf{D}^{(F)}\end{pmatrix}. \tag{18}$$

Here, by $\mathbf{D}^{(S)}$ [$\mathbf{D}^{(F)}$] we denoted submatrices of the dynamical matrix $\mathbf{D}$ which represent interaction of atoms inside L_S (L_F), and interaction between L_S and L_F is represented by the submatrices $\mathbf{D}^{(SF)}$ and $\mathbf{D}^{(FS)}$.

From Eqs. (3), (10), and (12) it follows that the total Hamiltonian of the system is

$$H_T = H_S(\mathbf{q},\mathbf{p}) + \tfrac{1}{2}\dot{\mathbf{u}}\cdot\dot{\mathbf{u}} + \tfrac{1}{2}\mathbf{u}\cdot\mathbf{D}\mathbf{u} + \Phi_0(\mathbf{q}) + \mathbf{f}(\mathbf{q})\cdot\mathbf{u}^{(S)} + \tfrac{1}{2}\mathbf{u}^{(S)}\cdot\mathbf{G}(\mathbf{q})\mathbf{u}^{(S)}. \tag{19}$$

In our formulation we neglect the last term in Eq. (19), because coupling between atoms of the zeolite crystal (covalent bond) is usually much stronger than the coupling between the sorbate molecule and zeolite atoms (van der Waals interaction), hence the lattice vibration amplitude is small. This assumption of linear coupling between lattice vibration and the sorbate motion might fail in some systems when a sorbate molecule fits extremely tight in a bottleneck of a zeolite lattice, thus yielding a zeolite–lattice interaction comparable in strength to that of the zeolite–zeolite covalent bonds. We discuss this situation in Sec. VI.

From Eq. (19), vibration of the zeolite lattice is described by

$$\ddot{\mathbf{u}}^{(S)} = -\mathbf{D}^{(S)}\mathbf{u}^{(S)} - \mathbf{f}(\mathbf{q}) - \mathbf{h}^{(S)}, \tag{20}$$

$$\ddot{\mathbf{u}}^{(F)} = -\mathbf{D}^{(F)}\mathbf{u}^{(F)} - \mathbf{h}^{(F)}. \tag{21}$$

Interaction between L_S and L_F is described by the terms $\mathbf{h}^{(S)}$ and $\mathbf{h}^{(F)}$,

$$\mathbf{h}^{(S)} = \mathbf{D}^{(SF)}\mathbf{u}^{(F)},\ \mathbf{h}^{(F)} = \mathbf{D}^{(FS)}\mathbf{u}^{(S)}, \tag{22}$$

whereas the influence of the sorbate on lattice vibration is given by the term $\mathbf{f}$ in Eq. (20).

Equations (20) and (21) contain a complete description of motion of all zeolite atoms. However, we are only interested in the effect of the lattice vibration on the sorbate motion and hence we only need to consider motion of atoms in L_S in detail. In contrast, some averaged description for L_F is adequate. This can be achieved if we consider L_F as a thermal bath and assume that the only effect of interaction between atoms of L_F and L_S is to keep the atoms of L_S in

thermal equilibrium. Thus, we omit the terms **h** which explicitly describe this interaction and instead require thermal equilibrium for all $\mathbf{u}^{(S)}$ and $\dot{\mathbf{u}}^{(S)}$,

$$\mathrm{Prob}\{\mathbf{u}^{(S)},\dot{\mathbf{u}}^{(S)}\}\propto e^{-H/k_BT}, \tag{23}$$

where k_B is the Boltzmann constant and T is temperature. The total Hamiltonian H now contains only the sorbate and zeolite atoms in L_S and is given by

$$H=H_S(\mathbf{q},\mathbf{p})+\tfrac{1}{2}\dot{\mathbf{u}}^{(S)}\cdot\dot{\mathbf{u}}^{(S)}+\tfrac{1}{2}\mathbf{u}^{(S)}\cdot\mathbf{D}^{(S)}\mathbf{u}^{(S)} +\Phi_0(\mathbf{q})+\mathbf{f}(\mathbf{q})\cdot\mathbf{u}^{(S)}. \tag{24}$$

We expand $\mathbf{u}^{(S)}$ in terms of eigenvectors of the dynamical matrix $\mathbf{D}^{(S)}$ which is symmetric and positive definite and hence its eigenvalues ω_j^2 are positive and its eigenvectors $\mathbf{e}(j)$ can be chosen to be orthonormal in the key eigenvalue problem below:

$$\mathbf{D}^{(S)}\mathbf{e}(j)=\omega_j^2\mathbf{e}(j),\quad \mathbf{e}(i)\cdot\mathbf{e}(j)=\delta_{ij}. \tag{25}$$

Since the bonds between L_F and L_S are assumed to be unstretched by deterministic coupling dynamics with the sorbate, the vibration modes in L_S are allowed to propagate into L_F while the thermal vibrations of L_F only serve as stochastic thermostating of atoms in L_S (see Fig. 2). There is no reflection or feedback back into L_S. Each mode of Eq. (25) corresponds to a lattice vibration mode involving atoms defined by the eigenvector $\mathbf{e}(i)$ with frequency ω_i. We then use the eigenvectors of the dynamical matrix $\mathbf{D}^{(S)}$ as the basis for the lattice displacement vector and the dynamic force

$$\mathbf{u}^{(S)}=\sum_j Q_j\mathbf{e}(j),\ Q_j=\mathbf{u}^{(S)}\cdot\mathbf{e}(j),$$
$$\mathbf{f}(\mathbf{q})=\sum_j \varphi_j(\mathbf{q})\mathbf{e}(j),\ \varphi_j(\mathbf{q})=\mathbf{f}(\mathbf{q})\cdot\mathbf{e}(j). \tag{26}$$

In these new coordinates we obtain the following expression for the Hamiltonian:

$$H=H_S(\mathbf{q},\mathbf{p})+\frac{1}{2}\sum_j[\dot{Q}_j^2+\omega_j^2Q_j^2]+\Phi_0(\mathbf{q})+\sum_j\varphi_j(\mathbf{q})Q_j. \tag{27}$$

Thus, L_S is described by the following equation for each lattice vibrational mode:

$$\ddot{Q}_j=-\omega_j^2Q_j-\varphi_j(\mathbf{q}), \tag{28}$$

and the equations of motion for the sorbate are

$$\dot{\mathbf{q}}=\mathbf{A}^{-1}\mathbf{p}, \tag{29}$$

$$\dot{\mathbf{p}}=-\frac{1}{2}\mathbf{p}\nabla\mathbf{A}^{-1}(\mathbf{q})\mathbf{p}-\nabla U(\mathbf{q})-\nabla\Phi_0(\mathbf{q})-\sum_j\nabla\varphi_j(\mathbf{q})Q_j. \tag{30}$$

We solve the linear lattice vibration Eq. (28) to obtain

$$Q_j(t)=\frac{1}{\omega_j^2}\left.\frac{\partial H}{\partial Q_j}\right|_{t=0}\cos\omega_jt+\frac{1}{\omega_j}\left.\frac{\partial H}{\partial\dot{Q}_j}\right|_{t=0}\sin\omega_jt -\frac{1}{\omega_j^2}\varphi_j(\mathbf{q}(t))+\frac{1}{\omega_j^2}\int_0^t\nabla\varphi_j(\mathbf{q}(s))\cdot\dot{\mathbf{q}}(s) \times\cos[\omega_j(t-s)]ds, \tag{31}$$

and note that both Eqs. (28) and (31) are inappropriate in the limit of $\omega_j\to 0$.

Substituting this solution into Eq. (29), one obtains the generalized Langevin equation for the sorbate,

$$\dot{\mathbf{p}}=-\frac{1}{2}\mathbf{p}\nabla\mathbf{A}^{-1}(\mathbf{q})\mathbf{p}-\nabla U(\mathbf{q})-\nabla\Phi_{\mathrm{eff}}(\mathbf{q}) -\int_0^t\eta(\mathbf{q}(t),\mathbf{q}(s),t-s)\dot{\mathbf{q}}(s)ds+\mathbf{F}(\mathbf{q}(t),t), \tag{32}$$

where

$$\Phi_{\mathrm{eff}}(\mathbf{q})=\Phi_0(\mathbf{q})+\Delta\Phi(\mathbf{q}),\ \Delta\Phi(\mathbf{q})=-\frac{1}{2}\sum_j\frac{1}{\omega_j^2}\varphi_j^2(\mathbf{q}) \tag{33}$$

is the effective sorbate–lattice interaction potential. The stochastic forcing arises from the dynamic lattice vibration force such that

$$\eta(\mathbf{q}(t),\mathbf{q}(s),t-s)=\sum_j\frac{\cos[\omega_j(t-s)]}{\omega_j^2}\nabla\varphi_j(\mathbf{q}(t))\nabla\varphi_j(\mathbf{q}(s)) \tag{34}$$

is the memory friction kernel and

$$\mathbf{F}(\mathbf{q}(t),t)=-\sum_j\nabla\varphi_j(\mathbf{q}) \times\left\{\frac{\cos\omega_jt}{\omega_j^2}\left.\frac{\partial H}{\partial Q_j}\right|_{t=0}+\frac{\sin\omega_jt}{\omega_j}\left.\frac{\partial H}{\partial\dot{Q}_j}\right|_{t=0}\right\} \tag{35}$$

is the stochastic random force.

Remembering that lattice vibration modes in L_S are in equilibrium, i.e.,

$$\mathrm{Prob}\{Q_j,\dot{Q}_j\}\propto e^{-H/k_BT}, \tag{36}$$

we obtain

$$\langle\mathbf{F}(t)\rangle=0, \tag{37}$$

$$\langle\mathbf{F}(t)\mathbf{F}(s)\rangle=k_BT\eta(\mathbf{q}(t),\mathbf{q}(s),t-s). \tag{38}$$

The last equation is the fluctuation–dissipation theorem which relates the intensity of the noise to the friction tensor. Note that the harmonic approximation for lattice vibration and Boltzmann distribution, Eq. (36), of the vibration modes lead to the Gaussian distribution of the stochastic force and hence the statistical properties of the latter are completely specified by its average and variance, as given by Eqs. (37) and (38).

III. CRITERIA FOR IMPORTANCE OF LATTICE VIBRATION

The goal of this section is to estimate the position-dependent friction term η and the correction $\Delta\Phi$ to the potential energy due to lattice vibration. The memory friction tensor η can have a complicated dependence on the previous states of the system. However, since here we are only interested in order-of-magnitude estimates, we assume an exponential dependence for the two-time correlation of the friction term to capture the decorrelation by only one parameter,

$$\eta(\mathbf{q}(t),\mathbf{q}(s),t-s)=\mathbf{\Gamma}(\mathbf{q}(t))\exp(-|t-s|/\tau), \tag{39}$$

where τ is some correlation time and $\mathbf{\Gamma}(\mathbf{q}(t))=\eta(\mathbf{q}(t),\mathbf{q}(t),0)$ is the noise amplitude from Eq. (34) with $t=s$. This assumption allows us to reduce the generalized Langevin Eq. (32) to a Langevin equation with Markovian noise by introducing an auxiliary variable,[13]

$$\mathbf{z}=\mathbf{q}-\mathbf{\Gamma}^{-1}\int_0^t \eta(t-s)\dot{\mathbf{q}}(s)ds+\mathbf{\Gamma}^{-1}\mathbf{F}(t). \tag{40}$$

Then Eq. (32) is equivalent to equations

$$\dot{\mathbf{p}}=-\tfrac{1}{2}\mathbf{p}\nabla\mathbf{A}^{-1}(\mathbf{q})\mathbf{p}-\nabla U(\mathbf{q})-\nabla\Phi_{\text{eff}}-\mathbf{\Gamma}(\mathbf{q})(\mathbf{q}-\mathbf{z}), \tag{41}$$

$$\tau\dot{\mathbf{z}}=(\mathbf{q}-\mathbf{z})+\mathbf{\Gamma}^{-1}\mathbf{N}(t). \tag{42}$$

The new random force $\mathbf{N}(t)$ is Gaussian, has zero-mean and zero-correlation time,

$$\langle\mathbf{N}(t)\rangle=0,\langle\mathbf{N}(t)\mathbf{N}(s)\rangle=2k_BT\mathbf{\Gamma}(\mathbf{q}(t))\tau\delta(t-s), \tag{43}$$

and is related to $\mathbf{F}(t)$ by

$$\mathbf{N}(t)=\mathbf{F}(t)+\tau\dot{\mathbf{F}}(t). \tag{44}$$

From Eq. (41) it is clear that the effects of lattice vibration are negligible for a sorbate configuration $\mathbf{q}$ if

$$\mu(\mathbf{q})=\left|\frac{\Delta\Phi(\mathbf{q})}{\Phi_0(\mathbf{q})}\right|\ll 1 \tag{45}$$

and $\|\mathbf{\Gamma}(\mathbf{q})(\mathbf{q}-\mathbf{z})\|\ll\|\nabla\Phi_0(\mathbf{q})\|$, where $\|\cdot\|$ is some vector norm (for definiteness we use the Euclidean norm). The latter condition is equivalent to

$$\nu(\mathbf{q})=\frac{\|\mathbf{\Gamma}(\mathbf{q})\|}{\|\nabla\nabla\Phi_0(\mathbf{q})\|}\ll 1. \tag{46}$$

Note that the conditions in Eqs. (45) and (46) are independent of the correlation time τ.

The computation of $\mu(\mathbf{q})$ and $\nu(\mathbf{q})$ is simplified if we take into account the pairwise additivity, Eq. (15), of the sorbate–zeolite interaction potential Φ to obtain

$$\varphi_j(\mathbf{q})=-\sum_{\mathbf{l}\kappa\in L_S}\sum_{s}^{N}\sum_{\alpha=1}^{3} m_\kappa^{-1/2}\left.\frac{\partial\phi_{s\kappa}(\mathbf{X})}{\partial X_\alpha}\right|_{\mathbf{X}=\mathbf{X}_s-\mathbf{r}_0(\mathbf{l}\kappa)} \times e_\alpha(\mathbf{l}\kappa;j). \tag{47}$$

Thus defining

$$v_\alpha(\mathbf{l}\kappa;\mathbf{q})=\sum_s^N\left.\frac{\partial\phi_{s\kappa}(\mathbf{X})}{\partial X_\alpha}\right|_{\mathbf{X}=\mathbf{X}_s-\mathbf{r}_0(\mathbf{l}\kappa)}, \tag{48}$$

$$w_\alpha(\mathbf{l}\kappa;\mathbf{q},i)=\sum_s^N\sum_{\beta=1}^{3}\left.\frac{\partial^2\phi_{s\kappa}(\mathbf{X})}{\partial X_\alpha\partial X_\beta}\right|_{\mathbf{X}=\mathbf{X}_s-\mathbf{r}_0(\mathbf{l}\kappa)}\frac{\partial X_{s\beta}}{\partial q_i}, \tag{49}$$

$$S_{\alpha\beta}(\mathbf{l}\kappa,\mathbf{l}'\kappa')=(m_\kappa m_{\kappa'})^{-1/2}\sum_j\frac{e_\alpha(\mathbf{l}\kappa,j)e_\beta(\mathbf{l}'\kappa',j)}{\omega_j^2}, \tag{50}$$

we obtain

$$\Delta\Phi(\mathbf{q})=-\frac{1}{2}\sum_{\mathbf{l}\kappa}\sum_{\mathbf{l}'\kappa'}\sum_{\alpha,\beta=1}^{3} v_\alpha(\mathbf{l}\kappa;\mathbf{q})S_{\alpha\beta}(\mathbf{l}\kappa,\mathbf{l}'\kappa') \times v_\beta(\mathbf{l}'\kappa';\mathbf{q}), \tag{51}$$

$$\Gamma_{ij}(\mathbf{q})=\sum_{\mathbf{l}\kappa}\sum_{\mathbf{l}'\kappa'}\sum_{\alpha,\beta=1}^{3} w_\alpha(\mathbf{l}\kappa;\mathbf{q},i)S_{\alpha\beta}(\mathbf{l}\kappa,\mathbf{l}'\kappa') \times w_\beta(\mathbf{l}'\kappa';\mathbf{q},j),\quad i,j=1,\ldots,N. \tag{52}$$

Or, in more compact form,

$$\Delta\Phi(\mathbf{q})=-\tfrac{1}{2}\mathbf{v}(\mathbf{q})\cdot\mathbf{S}\mathbf{v}(\mathbf{q}), \tag{53}$$

$$\Gamma_{ij}(\mathbf{q})=\mathbf{w}(\mathbf{q},i)\cdot\mathbf{S}\mathbf{w}(\mathbf{q},j),\quad i,j=1,\ldots,N. \tag{54}$$

The contributions of lattice vibration to the effective potential and the stochastic noise are hence contained in the tensor $\mathbf{S}$ which is a frequency-weighted dyadic product of the eigenvectors of the dynamical matrix $\mathbf{D}^{(S)}$.

IV. COMPARISON TO PERIODIC LATTICE

The separation of the lattice atoms into L_S and L_F is an important departure from the earlier work on lattice vibration.[4] As we have seen in Eq. (34), the magnitude of interaction between a sorbate and a vibrational mode of frequency ω_j is proportional to ω_j^{-2}. Thus, the dominant contribution to this interaction is due to vibrational modes with small frequencies. If, as in Ref. 4, all the modes are kept in the formulation then the dominant contribution is due to long acoustic modes[14] for which $\omega(\mathbf{k})\to 0$ as $\mathbf{k}\to 0$ ($\mathbf{k}$ is a wave vector). This is not physical as a single sorbate molecule cannot excite a macroscopic sound wave in an unbounded medium.

The problem with this formulation is that the quadratic terms in Eq. (12) are neglected and these terms actually become important when $\omega_j\to 0$. To see this, we rewrite Eq. (27) and keep the quadratic terms in Q_j,

$$H=H_S(\mathbf{q},\mathbf{p})+\frac{1}{2}\sum_j[\dot{Q}_j^2+\omega_j^2Q_j^2]+\Phi_0(\mathbf{q}) +\sum_j\varphi_j(\mathbf{q})Q_j.+\frac{1}{2}\sum_{i,j}\psi_{ij}(\mathbf{q})Q_iQ_j, \tag{55}$$

where

$$\psi_{ij}(\mathbf{q})=\mathbf{e}(i)\cdot\mathbf{G}(\mathbf{q})\mathbf{e}(j). \tag{56}$$

Due to orthonormality of vectors $\mathbf{e}(j)$, the matrix $\mathbf{\Psi}(\mathbf{q})$ has the same eigenvalues as $\mathbf{G}(\mathbf{q})$, which are the frequencies of sorbate vibrations in the well of the Lennard-Jones potential, whereas $\omega_j\to 0$ for acoustic modes. Thus, for acoustic modes, quadratic in Q terms due to the lattice–sorbate inter-

action [the last term in Eq. (55)] are larger than those due to the free lattice vibration [the third term in Eq. (55)].

To be consistent, one would need to include nonlinear interactions in the model, which will complicate the analysis, as nonlinear lattice vibration would yield localized wave packets[9] that do not behave stochastically. The lattice would then behave not as a thermal bath but as an active dynamic participant — an unlikely scenario in a macroscopic medium. Moreover, nonlinear lattice vibration tends to form localized wave packets which would pass by the sorbate rapidly, further reducing their interaction. The only possibility then is that the long acoustic modes are never at sufficiently large amplitude to require a nonlinear treatment. Simulations that yield large acoustic vibration must be due to feedback from the artificial periodic lattice model. The most realistic model is hence to cut off these long acoustic modes while still retaining the linear lattice model.

The above arguments suggest that a periodic lattice artificially excites long acoustic modes. This is further supported by the observation that finite-size periodic lattices have only discrete eigenmodes, including ones with zero frequencies due to the periodicity assumption, which further exaggerates the presence of low-frequency acoustic modes and leads to a resonant enhancement of standing acoustic waves. Specifically, the dynamics for the zero-frequency mode cannot be described by Eq. (28) as its solution, Eq. (31), becomes singular as ω_j vanishes. In order to describe this situation, let us briefly review the theory of periodic lattice vibration[14] and derive the amplitude equations of the zero-frequency modes.

Assume that the crystal is composed of periodically-repeated blocks of $L_1\times L_2\times L_3$ unit cells. This allows one to define a Fourier transform $\hat{\mathbf{u}}(\mathbf{k})$ of atom displacements $\mathbf{u}$,

$$u_\alpha(\mathbf{l}\kappa)=(L_1L_2L_3)^{-1/2}\sum_{\mathbf{k}}\hat{u}_\alpha(\kappa;\mathbf{k})e^{i\mathbf{k}\cdot\mathbf{r(l)}}, \tag{57}$$

$$\hat{u}_\alpha(\kappa;\mathbf{k})=(L_1L_2L_3)^{-1/2}\sum_{\mathbf{l}}u_\alpha(\mathbf{l}\kappa)e^{-i\mathbf{k}\cdot\mathbf{r(l)}}. \tag{58}$$

Here $l_i=1,\ldots,L_i$ $(i=1,2,3)$, $\alpha=1,2,3$, and $\mathbf{k}$ is a wave vector of the reciprocal lattice given by

$$\mathbf{k}=\frac{h_1}{L_1}\mathbf{b_1}+\frac{h_2}{L_2}\mathbf{b_2}+\frac{h_3}{L_3}\mathbf{b_3},\ h_i=1,\ldots,L_i,\ i=1,2,3, \tag{59}$$

with $\mathbf{b_1}$, $\mathbf{b_2}$, $\mathbf{b_3}$ being a basis of the reciprocal lattice, $\mathbf{a_i}\cdot\mathbf{b_j}=\mathbf{2}\pi\delta_{\mathbf{ij}}$.

The Fourier transform $\hat{\mathbf{D}}(\mathbf{k})$ of the dynamical matrix $\mathbf{D}$ is

$$\hat{D}_{\alpha\beta}(\kappa\kappa';\mathbf{k})=\sum_{\mathbf{l}'}D_{\alpha\beta}(\mathbf{l}\kappa,\mathbf{l}'\kappa')e^{-i\mathbf{k}\cdot\mathbf{r(l-l')}}, \tag{60}$$

and is independent of $\mathbf{l}$ since $D_{\alpha\beta}(\mathbf{l}\kappa,\mathbf{l}'\kappa')$ depends on $\mathbf{l}$ only through the difference $(\mathbf{l}-\mathbf{l}')$. The total Hamiltonian becomes

$$H_T=H_S(\mathbf{q},\mathbf{p})+\frac{1}{2}\sum_{\mathbf{k}}[\dot{\hat{\mathbf{u}}}^*(\mathbf{k})\cdot\dot{\hat{\mathbf{u}}}(\mathbf{k})+\hat{\mathbf{u}}^*(\mathbf{k})\cdot\hat{\mathbf{D}}(\mathbf{k})\hat{\mathbf{u}}(\mathbf{k})]$$
$$+\Phi_0(\mathbf{q})+\sum_{\mathbf{k}}\hat{\mathbf{f}}^*(\mathbf{k},\mathbf{q})\cdot\hat{\mathbf{u}}(\mathbf{k}), \tag{61}$$

where star denotes complex conjugation and

$$\hat{f}_\alpha(\kappa;\mathbf{k},\mathbf{q})=(L_1L_2L_3)^{-1/2}\sum_{\mathbf{l}}f_\alpha(\mathbf{l}\kappa,\mathbf{q})e^{-i\mathbf{k}\cdot\mathbf{r(l)}} \tag{62}$$

is the Fourier transform of $\mathbf{f}$.

The infinite crystal is recovered in the limit $L_1,L_2,L_3\to\infty$, in which case, the wave vector $\mathbf{k}$ takes continuous values and the sums in Eq. (61) are replaced by integrals. Note that an accurate description based on the periodic boundary conditions inherently requires infinitely many Fourier modes since one needs high resolution of the Fourier transform in order to describe behavior of very localized disturbances of lattice vibration due to the presence of a sorbate. However, in most MD simulations a very small size of a periodic simulation box — typically, a few unit cells — is assumed and below we describe the drawback of this assumption.

For simplicity, we consider transport of a point–mass sorbate in a periodic box consisting of a single unit cell. In this case, the only allowed value for the wave vector $\mathbf{k}$ is zero and the Fourier transforms, Eqs. (58), (60), (62), simplify to

$$\hat{u}_\alpha(\kappa)=u_\alpha(\mathbf{l}\kappa),\ \hat{f}_\alpha(\kappa;\mathbf{q})=f_\alpha(\mathbf{l}\kappa,\mathbf{q}), \tag{63}$$

$$\hat{D}_{\alpha\beta}(\kappa,\kappa')=\sum_{\mathbf{l}'}D_{\alpha\beta}(\mathbf{l}\kappa,\mathbf{l}'\kappa'), \tag{64}$$

where we write $\hat{\mathbf{u}}$, $\hat{\mathbf{f}}(\mathbf{q})$ and $\hat{\mathbf{D}}$ instead of $\hat{\mathbf{u}}(\mathbf{0})$, $\hat{\mathbf{f}}(\mathbf{0},\mathbf{q})$, and $\hat{\mathbf{D}}(\mathbf{0})$, respectively. The Hamiltonian, Eq. (61), can now be rewritten as

$$H_T=H_S(\mathbf{q},\mathbf{p})+\Phi_0(\mathbf{q})+\tfrac{1}{2}[\dot{\hat{\mathbf{u}}}\cdot\dot{\hat{\mathbf{u}}}+\hat{\mathbf{u}}\cdot\hat{\mathbf{D}}\hat{\mathbf{u}}]+\hat{\mathbf{f}}(\mathbf{q})\cdot\hat{\mathbf{u}}. \tag{65}$$

Following the same path as in Sec. II, we write

$$\hat{\mathbf{u}}=\sum_{j=1}^{3n}\hat{Q}_j\hat{\mathbf{e}}(j),\ \hat{Q}_j=\hat{\mathbf{u}}\cdot\hat{\mathbf{e}}(j), \tag{66}$$

$$\hat{\mathbf{f}}(\mathbf{q})=\sum_{j=1}^{3n}\hat{\varphi}_j(\mathbf{q})\hat{\mathbf{e}}(j),\ \hat{\varphi}_j(\mathbf{q})=\hat{\mathbf{f}}(\mathbf{q})\cdot\hat{\mathbf{e}}(j), \tag{67}$$

where $\hat{\mathbf{e}}(j)$ are the eigenvectors of the $3n\times3n$ symmetric positive-definite matrix $\hat{\mathbf{D}}$,

$$\hat{\mathbf{D}}\hat{\mathbf{e}}(j)=\hat{\omega}_j^2\hat{\mathbf{e}}(j),\ \hat{\mathbf{e}}(i)\cdot\hat{\mathbf{e}}(j)=\delta_{ij}. \tag{68}$$

The Hamiltonian, Eq. (65), can be written as

$$H_T=\frac{1}{2}M\dot{X}^2+\frac{1}{2}\sum_{j=1}^{3n}[\dot{\hat{Q}}_j^2+\hat{\omega}_j^2\hat{Q}_j^2]+\Phi_0(\mathbf{X})$$
$$+\sum_{j=1}^{3n}\hat{\varphi}_j(\mathbf{X})\hat{Q}_j, \tag{69}$$

where we take into account that the sorbate is a point–mass particle.

The matrix $\hat{\mathbf{D}}$ has three zero eigenvalues, $\omega_j=0$ for $j=1,2,3$ which is a consequence of the invariance of the periodic lattice vibration to uniform translation of the crystal.[14]

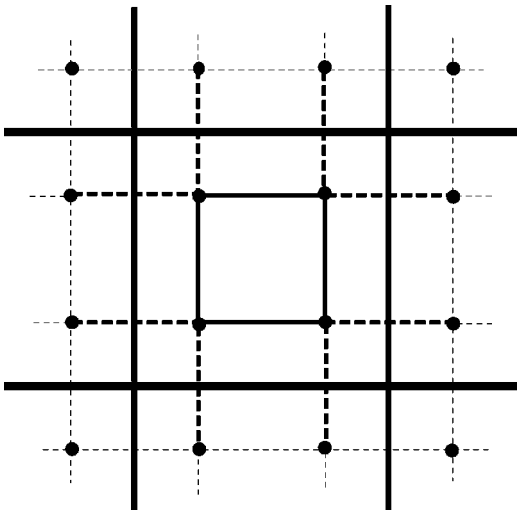

FIG. 3. Comparison of definitions of $\mathbf{D}^{(S)}$ and $\hat{\mathbf{D}}$ when L_S coincides with a zeolite unit cell. Matrix $\mathbf{D}^{(S)}$ includes only the bonds inside L_S (solid lines) whereas matrix $\hat{\mathbf{D}}$ contains these latter bonds as well as the bonds that connect atoms inside and outside of the unit cell (thick broken lines).

To see this, observe that, from Eq. (7), the αth component of the force exerted on the $(\mathbf{l}\kappa)$th atom of a freely vibrating (i.e., noninteracting with a sorbate) lattice is

$$-\frac{\partial H_L}{\partial r_\alpha(\mathbf{l}\kappa)}=-\sum_{\mathbf{l}'\kappa'}\sum_{\beta=1}^{3} V_{\alpha\beta}(\mathbf{l}\kappa,\mathbf{l}'\kappa')\rho_\beta(\mathbf{l}'\kappa'). \tag{70}$$

If we uniformly translate the crystal by an arbitrary vector $\mathbf{v}$, $\mathbf{r}(\mathbf{l}\kappa)\rightarrow\mathbf{r}(\mathbf{l}\kappa)+\mathbf{v}$, this force should not change. This constraint leads to

$$\sum_{\mathbf{l}'\kappa'}\sum_{\beta=1}^{3} V_{\alpha\beta}(\mathbf{l}\kappa,\mathbf{l}'\kappa')v_\beta=0. \tag{71}$$

This equation together with Eqs. (11) and (64) yields

$$\sum_{\kappa'} m_{\kappa'}^{1/2}\sum_{\mathbf{l}'} D_{\alpha\beta}(\mathbf{l}\kappa,\mathbf{l}'\kappa')=\sum_{\kappa'} m_{\kappa'}^{1/2}\hat{D}_{\alpha\beta}(\kappa,\kappa')=0, \tag{72}$$

and hence the matrix $\hat{\mathbf{D}}$ has three zero eigenvalues with the zero eigenspace spanned by vectors

$$\hat{e}_\alpha(\kappa,j)=\delta_{\alpha j}\left(\frac{m_\kappa}{m}\right)^{1/2},\ j=1,2,3, \tag{73}$$

where $m=\Sigma_{\kappa=1}^{n}m_\kappa$ is the total mass of atoms in a zeolite unit cell.

Note that the dynamical matrix $\mathbf{D}^{(S)}$ from our new model with cut off does not have these zero eigenvalues since our definition of this matrix breaks the translational symmetry:

$$D_{\alpha\beta}^{(S)}(\mathbf{l}\kappa,\mathbf{l}'\kappa')=D_{\alpha\beta}(\mathbf{l}\kappa,\mathbf{l}'\kappa')\neq\sum_{\mathbf{l}'} D_{\alpha\beta}(\mathbf{l}\kappa,\mathbf{l}'\kappa')$$
$$=\hat{D}_{\alpha\beta}(\kappa,\kappa'). \tag{74}$$

The situation is schematically illustrated in Fig. 3 where L_S is chosen to coincide with a zeolite unit cell. As can be seen, the matrices $\mathbf{D}^{(S)}$ and $\hat{\mathbf{D}}$ differ in that the latter does not include the bonds between zeolite atoms that belong to different unit cells — phonon modes are absorbed at these boundaries.

Since here we focus on interaction between the sorbate and acoustic modes, we keep only the three zero modes in the periodic Hamiltonian, Eq. (69):

$$H_T=\frac{1}{2}M\dot{X}^2+\frac{1}{2}\sum_{j=1}^{3}\dot{\hat{Q}}_j^2+\Phi_0(\mathbf{X})+\sum_{j=1}^{3}\hat{\varphi}_j(\mathbf{X})\hat{Q}_j. \tag{75}$$

Then taking into account the pairwise additivity of the potential, Eq. (15), we obtain

$$\hat{\varphi}_j(\mathbf{X})=\frac{1}{\sqrt{m}}\sum_\kappa\left(\frac{\partial\Phi(\mathbf{X},\{\mathbf{r}\})}{\partial r_j(\kappa)}\right)_0=-\frac{1}{\sqrt{m}}\frac{\partial\Phi_0(\mathbf{X})}{\partial X_j}, \tag{76}$$

and thus the equations of motion become

$$M\ddot{X}_i=-\frac{\partial\Phi_0}{\partial X_i}+\frac{1}{\sqrt{m}}\sum_{j=1}^{3}\frac{\partial^2\Phi_0}{\partial X_i\partial X_j}\hat{Q}_j, \tag{77}$$

$$\ddot{\hat{Q}}_j=\frac{1}{\sqrt{m}}\frac{\partial\Phi_0}{\partial X_j}. \tag{78}$$

The behavior of the acoustic modes governed by Eq. (78) shows a drastic difference from the behavior of modes with nonzero frequencies described by Eq. (28). The solution of Eq. (78),

$$\hat{Q}_j(t)=\hat{Q}_j(0)+\dot{\hat{Q}}_j(0)t+\frac{1}{\sqrt{m}}\int_0^t\int_0^s\frac{\partial\Phi_0(\mathbf{X}(s'))}{\partial X_j}ds'ds, \tag{79}$$

shows that sorbate motion induces a nonoscillatory motion of these acoustic waves both from the second and third terms in Eq. (79). The secular growth term arises from the degeneracy of the zero-frequency eigenvalues. It disappears for specific initial conditions. However, the third term represents energy accumulation due to periodicity and its effect is far stronger than the second term. It accumulates acoustic modes resonantly and indefinitely increases the amplitude of these waves — a patently impossible blow-up scenario. If this resonance growth is sustained indefinitely, the lattice will break apart and the sorbate will transport at unrealistically high rates. In contrast, the amplitude of modes with nonzero frequency given by Eq. (31) is oscillatory in time.

To observe the resonant growth of the acoustic modes, we solve the coupled Eqs. (77) and (78) numerically for xenon in zeolites sodalite and silicalite. The zeolite crystals are composed of TO_4 tetrahedra (T is Si or Al) and in this work we assume that T is always an Si atom. This allows us to neglect ionic intracrystalline interactions. We model zeolites using the structural data from the MSI CERIUS^2 software package.[15] For the zeolite lattice vibration, we use the following model of the interaction potential between zeolite atoms:[16]

$$V=\frac{1}{2}\sum K_r(r-r_0)^2+\frac{1}{2}\sum K_\alpha(\alpha-\alpha_0)^2$$
$$+\frac{1}{2}\sum K_\beta(\beta-\beta_0)^2, \tag{80}$$

TABLE I. Force constants used in Eq. (80).

T–O	$K_r = 2500$ kJ mol^{-1} Å^{-2}
O–T–O	$K_\alpha = 578$ kJ mol^{-1} rad^{-2}
T–O–T	$K_\beta = 75.9$ kJ mol^{-1} rad^{-2}

where r is the T–O distance, α is O–T–O angle, and β is T–O–T angle. The values of force constants K_r, K_α, K_β are given in Table I. The equilibrium bond length (r_0) and angles (α_0 and β_0) were calculated directly from the structural data.

As a check of our lattice model, we compute the infrared spectrum for zeolites sodalite and silicalite by solving the eigenvalue problem, Eq. (68), for the Fourier transform of the dynamical matrix at the zero wave vector $\mathbf{k}$ and then using the following formula for infrared intensity $I(\hat{\omega}_j)$ of jth vibration mode with frequency $\hat{\omega}_j$:[17]

$$I(\hat{\omega}_j) = \sum_{\alpha=1}^{3} \left(\sum_{\kappa} q_\kappa m_\kappa^{-1/2} \hat{e}_\alpha(\kappa, j) \right)^2, \tag{81}$$

where q_κ is the formal ionic charge of the κth atom and $\hat{\mathbf{e}}(\kappa, j)$ is the normalized displacement vector of the κth atom in the jth mode, i.e., it is the eigenvector of the dynamical matrix that corresponds to the eigenvalue $\hat{\omega}_j^2$. In our calculations we used $q_\kappa = -1.6$ for T atoms and $q_\kappa = -0.8$ for oxygen atoms.[16] The computed frequency spectra are shown in Figs. 4 and 5 and are in good agreement with experimental ones (since we limit ourselves to harmonic vibrations, the theoretical calculation of spectrum cannot resolve the width of the peaks since it is a manifestation of anharmonic effects).

Xenon molecules are modeled as point masses which interact with the lattice oxygen atoms via the Lennard-Jones potential,

$$\phi_{\mathrm{LJ}}(r) = 4\epsilon \left(\left(\frac{\sigma}{r} \right)^{12} - \left(\frac{\sigma}{r} \right)^{6} \right), \tag{82}$$

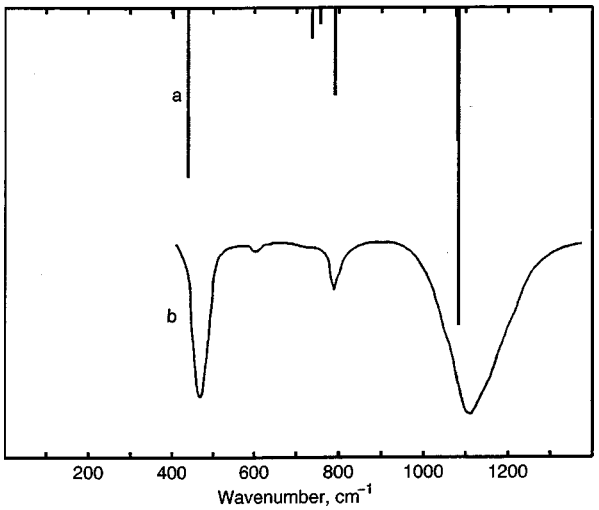

FIG. 4. Infrared spectrum of sodalite: (a) calculated, (b) experimental (Ref. 17).

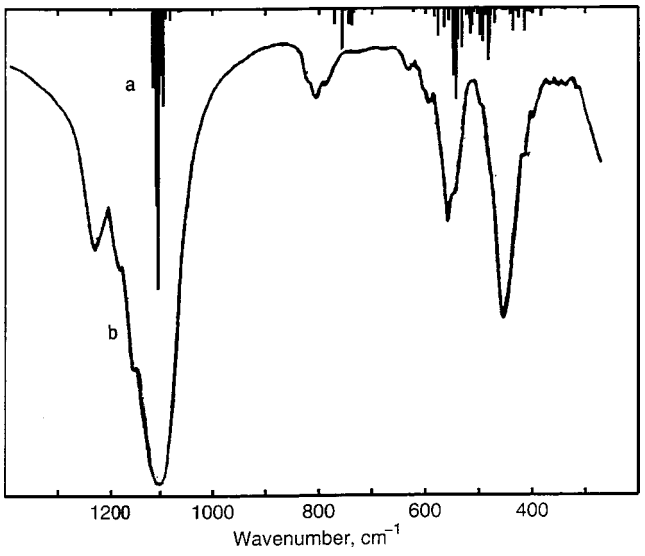

FIG. 5. Infrared spectrum of silicalite: (a) calculated, (b) experimental (Ref. 26).

where r is the distance between a zeolite oxygen atom and the sorbate. Values of the parameters ϵ and σ for xenon–oxygen interaction were taken from Ref. 18 and are given in Table II. As usual, the interaction between sorbates and the lattice T atoms is neglected, since the latter are shielded by the oxygen atoms in TO_4 tetrahedra.[19]

We simulate Eqs. (77) and (78) using the velocity Verlet algorithm.[20] Initial position for the xenon molecule is at a potential minimum, $\mathbf{X} = (0.280, 0.280, 8.610)$ for xenon in sodalite and $\mathbf{X} = (4.013, 4.975, 12.086)$ for xenon in silicalite (the coordinates are given in Å and the origin is located at a unit cell corner). Initial kinetic energy of the sorbate is chosen to be 11.331 kJ/mol and initial $\hat{Q}_j$ and $\dot{\hat{Q}}_j$ are zeros. This choice of initial conditions for $\hat{Q}_j$ and $\dot{\hat{Q}}_j$ eliminates the linear growth of $\hat{Q}_j$ due to the second term in Eq. (79) and focuses on resonant amplification due to the last term. The evolution of amplitudes of the acoustic modes $\hat{Q}_j$, obtained in our simulation of Eqs. (77) and (78) in Fig. 6 shows very rapid resonant enhancement of acoustic modes, which occurs due to the accumulation of the amplitude of acoustic modes. The same qualitative picture was obtained in simulations

TABLE II. Lennard-Jones parameters of interaction potential between sorbates and lattice oxygen.

	ϵ (J/mol)	σ (Å)
Methane[a]	1108.3	3.214
Neon[b]	529.0	2.780
Argon[b]	1028.0	3.029
Xenon[c]	1133.1	3.453
CH_3 (ethane)[d]	696.7	3.364
C (benzene)[e]	611.5	3.007
H (benzene)[e]	407.9	2.606

[a]Reference 6.
[b]Reference 25.
[c]Reference 18.
[d]Reference 22.
[e]Reference 23.

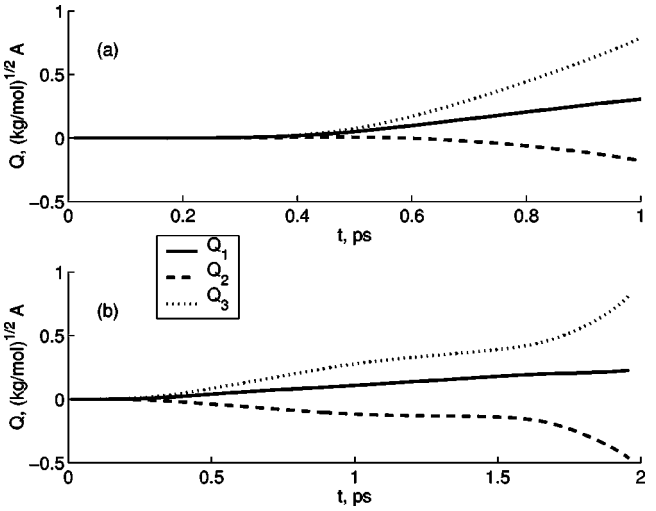

FIG. 6. Results of simulations of Eqs. (77), (78) for xenon in sodalite (a) and silicalite (b).

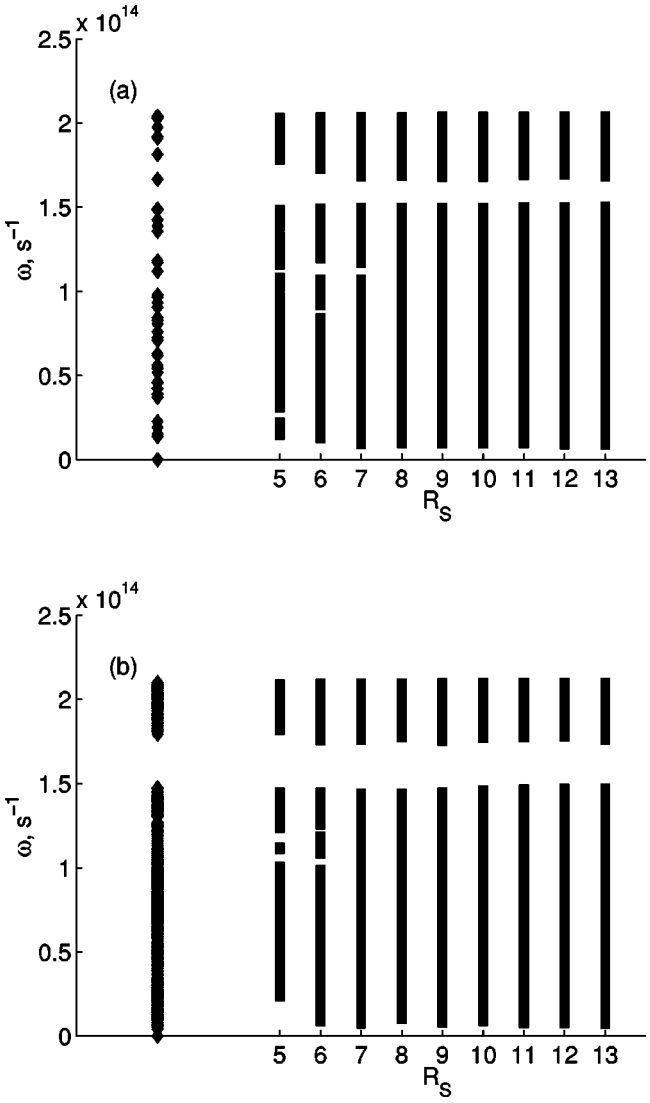

FIG. 7. Dependence of the vibration spectrum of $\mathbf{D}^{(S)}$ on the radius R_S of L_S: (a) sodalite, (b) silicalite. The frequencies become nearly continuous for L_S larger than 8 Å in radius but the spectrum has a lower cutoff of about $10^{13}\,\mathrm{s}^{-1}$. In contrast, the spectrum of $\hat{\mathbf{D}}(\mathbf{0})$ for an infinitely-large periodic lattice (shown on the left), contains zero frequency acoustic modes.

with other initial conditions. Essentially, there is an unphysical ''feedback'' of lattice vibration in the periodic unit cell. Our new approach is devoid of such kinds of problems since any phonon wave created by a sorbate that is radiated into L_F never comes back to L_S.

As a final remark, we note that some MD simulations which include lattice vibration and assume periodic boundary conditions do not report resonance blow-up. The explanation for this is that these MD simulations use a nonharmonic model for the lattice, even if the model is harmonic in terms of bond length stretching and bond angle bending, such as Eq. (80), it is anharmonic in terms of atom displacements $\mathbf{u}$ (since $\mathbf{u}$ is related nonlinearly to bond length stretching and bond angle bending). This anharmonicity then prevents sustained resonant growth of the acoustic waves. However, there is still unphysical feedback of the lattice vibration in these MD simulations with periodic boundary conditions such that unrealistically large saturated amplitudes are produced to drive sorbate at high rates. The validity of such simulations is questionable.

V. RESULTS

Now we are in a position to answer an important question: How sensitive is the above theory to a particular definition of L_S? To answer this question, we fix a position of a xenon sorbate in zeolites sodalite and silicalite and compute spectra of matrices $\mathbf{D}^{(S)}$ as well as μ and ν for different choices of L_S.

We define L_S as a sphere of radius R_S with center coinciding with the center-of-mass $\mathbf{X}$ of the sorbate and let R_S vary from 5 to 13 Å. The spectra of the matrices $\mathbf{D}^{(S)}$ for different R_S are shown in Fig. 7. Also, spectra of matrices $\hat{\mathbf{D}}(\mathbf{0})$ for the periodic lattice are shown there for comparison. As can be seen, the spectra for both zeolites become insensitive to R_S for $R_S \geqslant 8$ Å. This indicates that the most important lattice vibration modes that drive sorbate transport are shorter than 8 Å. Also note that the spectra of $\mathbf{D}^{(S)}$ are very similar to the spectra of $\hat{\mathbf{D}}(\mathbf{0})$ except the former do not have zero eigenvalues and other acoustic modes. The lowest frequency for our model lattice converges at about $10^{13}\,\mathrm{s}^{-1}$ for $R_S \geqslant 8$ Å. All other modes have higher frequencies and quickly approach a near continuum at large R_S. The results of the calculations for μ and ν are shown in Fig. 8 and suggest that values of $\mu(\mathbf{X})$ and $\nu(\mathbf{X})$ for $R_S \geqslant 8$ Å are also insensitive to the choice of R_S, thus supporting the validity of our model. Convergence beyond $R_S = 8$ Å indicates that the sorbate can only interact with local vibration of lattice atoms within 8 Å. Energy transfer to low-frequency, long-acoustic modes has been removed by our new lattice model. We hence use L_S with radius $R_S = 9$ Å in our calculations of $\mu(\mathbf{q})$ and $\nu(\mathbf{q})$ described below.

However, before proceeding with the calculations, we have to address another important issue, namely, a very strong dependence of $\mu(\mathbf{q})$ and $\nu(\mathbf{q})$ on sorbate configuration $\mathbf{q}$. In particular, μ and ν are usually relatively small for sorbates inside zeolite cages, whereas they become larger for

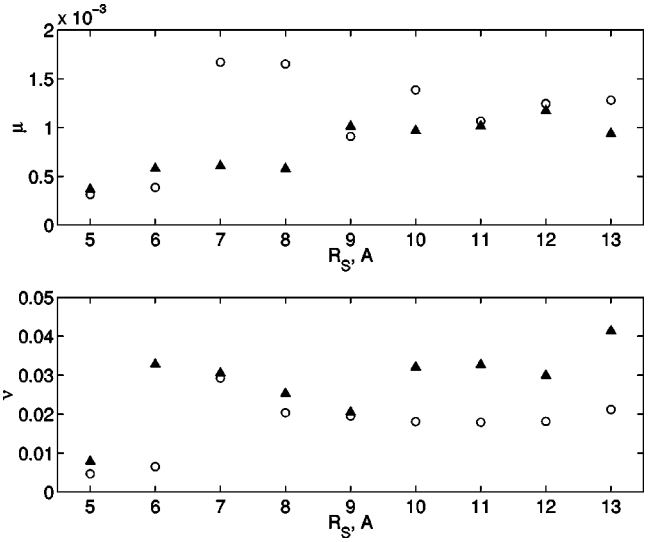

FIG. 8. Dependence of μ and ν on the radius R_S of L_S. Xenon in sodalite (○) at $\mathbf{X}=(0.280,0.280,8.610)$ and silicalite (▲) at $\mathbf{X}=(4.013,4.975,12.086)$ (coordinates are given in Å).

sorbates at bottlenecks of zeolite pores and they tend to infinity when sorbate approaches zeolite walls. Therefore, one has to be very careful about analyzing calculations of μ and ν.

It is tempting to calculate weighted averages $\langle\mu\rangle$ and $\langle\nu\rangle$, where

$$\langle\cdot\rangle=\frac{\int\cdot W(\mathbf{q})d\mathbf{q}}{\int W(\mathbf{q})d\mathbf{q}}, \tag{83}$$

and the weight $W(\mathbf{q})$ is the equilibrium Boltzmann distribution,

$$W(\mathbf{q})=e^{-[U(\mathbf{q})+\Phi_0(\mathbf{q})]/k_BT}. \tag{84}$$

Such an averaging will automatically ''filter out'' those configurations which correspond to sorbates located unphysically close to zeolite walls and hence having very high potential energy $\Phi_0(\mathbf{q})$. However, the Boltzmann averaging will also effectively eliminate narrow bottlenecks (i.e., high potential barriers) which sorbates have to transverse. Therefore, we have chosen a different approach, namely, we compute $\mu(\mathbf{q})$ and $\nu(\mathbf{q})$ at transition states of the potential energy (and also for comparison we compute these parameters at potential minima). The transition states as well as potential minima were obtained using the rational function optimization (RFO) algorithm of Banerjee *et al.*[21]

We compute μ and ν for methane, xenon, ethane, and benzene in silicalite and mordenite and for neon and argon in sodalite. Parameters for sorbate–zeolite interaction together with original references are summarized in Table II. Methane and inert gas molecules are modeled as point–masses which interact with lattice oxygen atoms via the Lennard-Jones potential, Eq. (82).

The models for ethane and benzene molecules were taken from Refs. 22 and 23, respectively. Ethane was modeled as a dumbbell consisting of two methyl groups connected by a rigid rod of length 1.53 Å. Each methyl group was modeled as a unified Lennard-Jones sphere interacting with the lattice via the potential, Eq. (82). An ethane molecule has five degrees of freedom with generalized coordinates $\mathbf{q}$ containing coordinates of the center-of-mass of the molecule and two Eulerian angles. We need only two Eulerian angles since ethane molecule is invariant under the rotation around the methyl–methyl bond.

TABLE III. Largest values of μ and ν computed at transition states of sorbate–zeolite systems with weak lattice noise.

	μ	ν
Methane in silicalite	1.4×10^{-3}	5.9×10^{-2}
Xenon in silicalite	7.2×10^{-4}	4.3×10^{-2}
Xenon in mordenite	1.8×10^{-3}	1.1×10^{-1}

Benzene was modeled as a planar rigid molecule with six degrees of freedom. Its generalized coordinates $\mathbf{q}$ are the center-of-mass coordinates and three Eulerian angles. The carbon–carbon and carbon–hydrogen bond lengths are 1.40 and 1.08 Å, respectively. The short-range interaction between benzene and zeolite lattice was modeled by the sum of pairwise Lennard-Jones interaction potentials between lattice oxygen and benzene carbon and hydrogen atoms. In the present work, we neglected long-range electrostatic interaction (due to quadrupole moment of a benzene molecule) between benzene and zeolite atoms.

We found that, depending on a particular sorbate–zeolite pair, effects of lattice vibration can be either very small or very large. For example, effects of lattice vibration are negligible for methane and xenon in silicalite and xenon in mordenite. The largest values of μ and ν computed at transition states of these systems are shown in Table III and confirm that the sorbate–lattice coupling is very weak.

Quite the opposite, a rather large sorbate–lattice coupling was found for benzene in silicalite and mordenite. In Figs. 9 and 10, we show μ and ν computed at potential barriers and minima of these system. For benzene in silicalite, μ and ν are order one quantities for most of the transition states and even for some minima. For benzene in

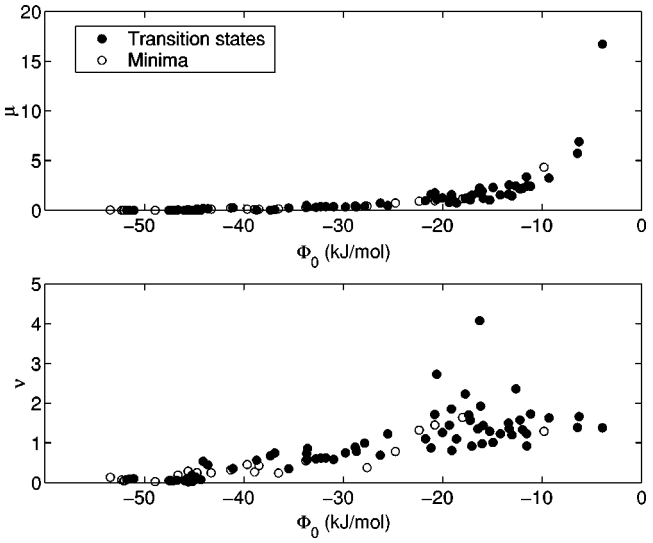

FIG. 9. Values of μ and ν for benzene in silicalite.

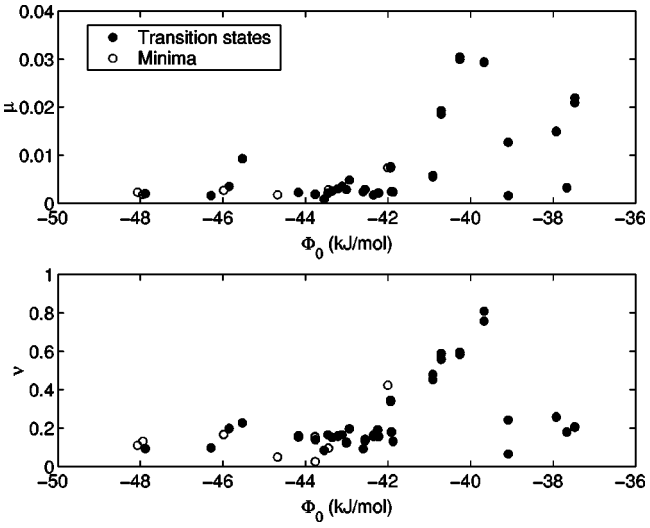

FIG. 10. Values of μ and ν for benzene in mordenite.

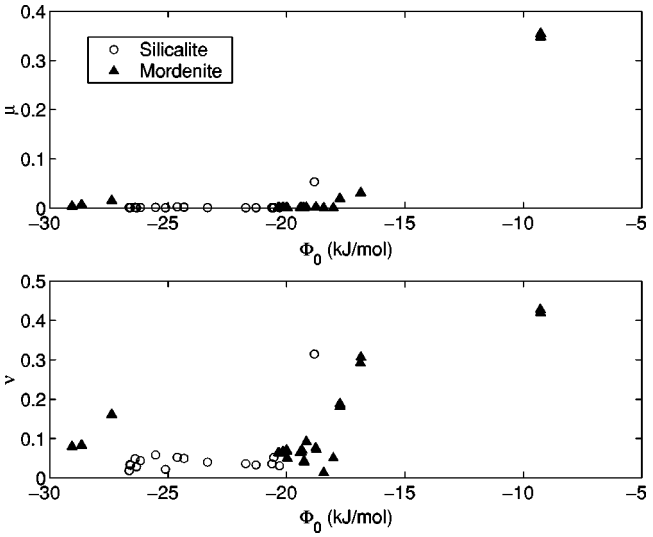

FIG. 12. Values of μ and ν computed for transition states of ethane in silicalite and mordenite.

mordenite, μ is small, but ν is still an order one quantity for a large number of transition states. Note that the sorbate–lattice coupling is larger for benzene in silicalite than for benzene in mordenite because the former zeolite has narrower pores that the latter.

Some of the considered sorbate–zeolite systems can incorporate both small and large noise cases due do the highly inhomogeneous structure of zeolite pores. Consider, for example, methane in mordenite. The mordenite crystal consists of straight pores and side pockets. In Fig. 11 we show a cross section of the mordenite channel at $x=9$ Å together with potential minima, transition states, and diffusion paths of the sorbate. As is evident, the methane sorbate can move either along the main channel (in which case it has to overcome the potential barrier at the point S_1) or the sorbate can hop from the main channel into a side pocket (in which case it has to go through a narrow bottleneck at the point S_2). At the point S_1, $\mu=1.0\times10^{-2}$ and $\nu=0.55\times10^{-1}$ whereas at the point S_2, $\mu=0.16$ and $\nu=0.34$. Thus, the coupling between the methane sorbate and lattice vibration is weak when the sorbate moves inside the main channel and it is quite large when the sorbate hops from the main channel to a side pocket.

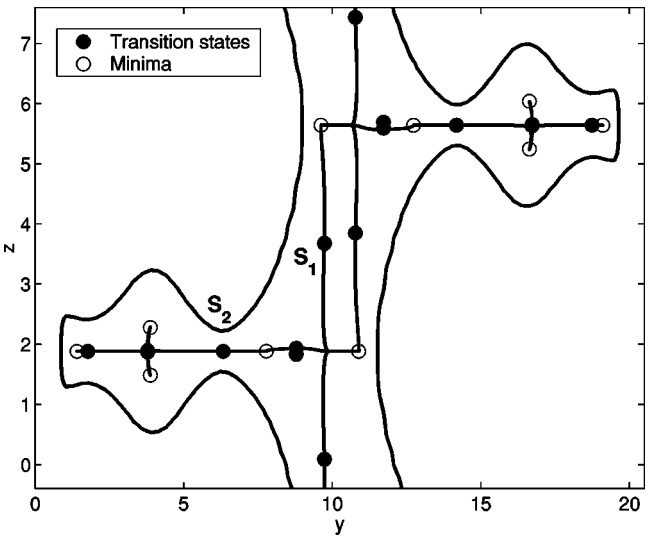

FIG. 11. Methane in mordenite. Cross section of the mordenite channel at $x=9$ Å. Potential minima, transition states, and diffusion paths of the sorbate are also shown. The sorbate–lattice coupling is negligible for diffusion along the main channel (through the S_1-type points) and is significant for hoppings between the main channel and the side pockets (through the S_2-type points).

Other examples of such mixed systems are ethane in silicalite and mordenite. Values of μ and ν computed at transition states of these systems are shown in Fig. 12. As can be seen, both of these systems have transition states with both weak and strong sorbate–lattice coupling. That is, motion of sorbates along some diffusion paths is driven by the lattice noise, and diffusion along others is driven by another mechanism.

Another interesting class of sorbate–zeolite pairs considered is inert gases in sodalite. It is known that, at high temperatures and pressures, these sorbates can be forced into the sodalite cages[5] and since the sodalite windows are narrower than the dimension of the sorbates, this can occur only if lattice vibration is permitted. More specifically, diffusion occurs only if the sorbate can open the window through local interaction. We considered neon and argon in sodalite and estimated our indices μ and ν at the transition state located in the six-ring cage window [see Fig. 1(a)]. Coordinates for this transition state are $\mathbf{X}=(2.16\ \text{Å}, 2.16\ \text{Å}, 2.16\ \text{Å})$ for both neon and argon. We found that for neon, $\mu(\mathbf{X})=4.8$, $\nu(\mathbf{X})=11.2$, and for argon, $\mu(\mathbf{X})=25.4$, $\nu(\mathbf{X})=62.3$. These results indicate that the lattice–sorbate interaction is extremely strong.

VI. DISCUSSION

We have seen that lattice noise can be an important driving force for some sorbate–zeolite systems while its effects are negligible in other systems. Diffusion driven by high noise is a well-studied process and is described in a classical article of Kramers.[24] However, for systems with weak lattice noise the lattice thermal bath is inefficient as a stochastic

fluctuation source and an energy sink for sorbates. The motion of these sorbates is then determined by driving forces other than lattice vibration. One possibility is that low-dimensional sorbate Hamiltonian dynamics can produce a deterministic but chaotic driving force even in a static lattice.[11] Without dissipation, the sorbate motion necessarily exhibits high inertial effects, with considerable rattling near potential minima. The crossing of the thresholds (pore necks) is then determined by how energy is transferred deterministically to the transverse degrees of freedom and regained at the threshold. This transfer between the degree of freedom in the diffusive direction with one in the transverse direction can be induced by nonaxisymmetric geometry in a pore and nonspherical geometry in a cage. It can be described as KAM chaos for coupled Hamiltonian systems and has been shown to give rise to seemingly random sorbate transport with diffusive statistics but not thermal in origin.[11]

There are two other possible driving forces for zeolite transport. One is when sorbate loading is sufficiently high such that significant clustering occurs due to sorbate–sorbate interaction along the narrow pores. However, lattice vibration would still be unimportant and the clustering dynamics remain deterministic and conservative. The clustering dynamics can conceivably be described by nonlinear sorbate concentration waves as in one-dimensional Toda waves.[9]

The other important possibility is when the rate-determining pore necks are narrower than the sorbate such that local lattice vibration is important. Our nonperiodic lattice model can capture these local dynamics that occur within $R_S = 8$ Å of the sorbate. However, since these vibrations triggered by the sorbate motion typically have large amplitude, they are intrinsically nonlinear. Hence, their resolution requires the quadratic terms in $\mathbf{u}^{(S)}$ in the zeolite–lattice interaction force, Eq. (12), that are omitted in the current model. The Hamiltonian, Eq. (24), of the sorbate–zeolite system then becomes

$$H = H_S(\mathbf{q},\mathbf{p}) + \tfrac{1}{2}\dot{\mathbf{u}}^{(S)}\cdot\dot{\mathbf{u}}^{(S)} + \tfrac{1}{2}\mathbf{u}^{(S)}\cdot\mathbf{D}^{(S)}\mathbf{u}^{(S)} + \Phi_0(\mathbf{q}) + \mathbf{f}(\mathbf{q})\cdot\mathbf{u}^{(S)} + \tfrac{1}{2}\mathbf{u}^{(S)}\cdot\mathbf{G}(\mathbf{q})\mathbf{u}^{(S)}, \tag{85}$$

and equation of motion for the atoms in L_S is

$$\ddot{\mathbf{u}}^{(S)} = -\mathbf{C}(\mathbf{q})\mathbf{u}^{(S)} - \mathbf{f}(\mathbf{q}), \tag{86}$$

where

$$C_{\alpha\beta}(\mathbf{l}\kappa,\mathbf{l}'\kappa';\mathbf{q}) = D^{(S)}_{\alpha\beta}(\mathbf{l}\kappa,\mathbf{l}'\kappa') + \delta_{\mathbf{l},\mathbf{l}'}\delta_{\kappa,\kappa'}G_{\alpha\beta}(\mathbf{l}\kappa,\mathbf{l}\kappa;\mathbf{q}). \tag{87}$$

Hence, the nonlinear lattice–sorbate interaction changes the frequencies of lattice atom vibration and this nonlinear interaction can only be neglected if the magnitude of these changes is small. To estimate the magnitude of this nonlinear correction, we compare eigenvalues of the matrices $\mathbf{D}^{(S)}$ and $\mathbf{C}(\mathbf{q})$ by computing the maximal relative deviation of eigenvalues $\lambda_j^C(\mathbf{q})$ of the matrix $\mathbf{C}(\mathbf{q})$ from the eigenvalues λ_j^D of the matrix $\mathbf{D}^{(S)}$,

$$\Delta\lambda(\mathbf{q}) = \max_j \left| \frac{\lambda_j^C(\mathbf{q}) - \lambda_j^D}{\lambda_j^D} \right|. \tag{88}$$

TABLE IV. Nonlinear corrections $\Delta\lambda$ computed at transition states.

	Silicalite	Mordenite	Sodalite
Methane	1.3×10^{-2}	8.1×10^{-2}	
Xenon	2.3×10^{-2}	4.2×10^{-2}	
Ethane	2.7×10^{-2}	8.5×10^{-2}	
Benzene	1.9×10^{-1}	1.8×10^{-1}	
Neon			2.2×10^{-1}
Argon			2.0

The quantity $\Delta\lambda(\mathbf{q})$ is well-defined and we have shown that its value converges with respect to the radius R_S of L_S for $R_S \geqslant 9$ Å. The maximal values of $\Delta\lambda$ at transition states are shown in Table IV. As can be seen, the nonlinear corrections are small for all zeolite–sorbate pairs considered except for argon in sodalite. This suggests that argon transport in sodalite is due entirely to highly nonlinear but localized interaction between argon and the window lattice atoms. Synchronization between the sorbate motion and the large-amplitude window dynamics is surely the dominant mechanism here.

These driving forces (intramolecular dynamics, Hamiltonian chaos, sorbate–sorbate interaction, stochastic linear and local nonlinear sorbate–lattice interactions) must be examined in detail to understand the peculiar dependence on loading and temperature. It appears, however, that diffusion of small sorbates through zeolite is not driven by lattice vibration or any other thermal noise. The lack of stochastic forcing also implies little dissipation and thus inertia must be important for small sorbate dynamics. As a result, diffusion of small sorbates through zeolite is a highly nonequilibrium process for which near-equilibrium theories, like the transition state theory, and the usual Arrhenius scaling are not applicable. Their MD simulation efforts require only a simple rigid lattice.

ACKNOWLEDGMENTS

This work is funded by grants from the Mobil Foundation and the Center for Applied Mathematics at the University of Notre Dame. We are grateful to E. J. Maginn for valuable input and for providing us access to his software.

[1] R. C. Runnebaum and E. J. Maginn, J. Phys. Chem. B **101**, 6394 (1997).
[2] W. Heink, J. Kärger, H. Pfeifer, and F. Stallmach, J. Am. Chem. Soc. **112**, 2175 (1990).
[3] R. Zwanzig, J. Stat. Phys. **9**, 215 (1973).
[4] R. Tsekov and E. Ruckenstein, J. Chem. Phys. **100**, 1450 (1994).
[5] R. M. Barrer and D. E. W. Vaughan, J. Phys. Chem. Solids **32**, 731 (1971).
[6] S. J. Goodbody, K. Watanabe, D. MacGowan, J. Walton, and N. Quirke, J. Chem. Soc., Faraday Trans. **87**, 1951 (1991).
[7] R. L. June, A. T. Bell, and D. N. Theodorou, J. Phys. Chem. **94**, 8232 (1990).
[8] P. Demontis, G. B. Suffritti, and P. Mura, Chem. Phys. Lett. **191**, 553 (1992).
[9] M. Toda, *Nonlinear Waves and Solitons* (Kluwer Academic, Dordrecht, 1989).
[10] W. M. Meier and D. H. Olson, *Atlas of Zeolite Structure Types*, 3rd ed. (Butterworth-Heinemann, London, 1992).
[11] D. I. Kopelevich and H.-C. Chang, Phys. Rev. Lett. **83**, 1590 (1999).
[12] G. Wahnstrom, K. Haug, and H. Metiu, Chem. Phys. Lett. **148**, 158

(1988); Z. Zhang, K. Haug, and H. Metiu, J. Chem. Phys. **93**, 3614 (1990); Z. Zhang and H. Metiu, *ibid*. **93**, 2087 (1990).
[13] E. Pollak and A. M. Berezhkovskii, J. Chem. Phys. **99**, 1344 (1993).
[14] A. A. Maradudin, E. W. Montroll, G. H. Weiss, and I. P. Ipatova, *Theory of Lattice Dynamics in the Harmonic Approximation* (Academic, New York, 1971).
[15] CERIUS2, Version 3.8, Molecular Simulations Inc., San Diego, CA, 1998.
[16] K. S. Smirnov and D. Bougeard, J. Phys. Chem. **97**, 9434 (1993).
[17] A. J. M. de Man and R. A. van Santen, Zeolites **12**, 269 (1992).
[18] R. L. June, A. T. Bell, and D. N. Theodorou, J. Phys. Chem. **95**, 8866 (1991).
[19] A. V. Kiselev, A. A. Lopatkin, and A. A. Shulga, Zeolites **5**, 261 (1985).
[20] W. C. Swope, H. C. Andersen, P. H. Berens, and K. R. Wilson, J. Chem. Phys. **76**, 637 (1982).
[21] A. Banerjee, N. Adams, J. Simons, and R. Shepard, J. Phys. Chem. **89**, 52 (1985).
[22] R. L. June, A. T. Bell, and D. N. Theodorou, J. Phys. Chem. **96**, 1051 (1992).
[23] R. Q. Snurr, A. T. Bell, and D. N. Theodorou, J. Phys. Chem. **98**, 11 948 (1994).
[24] H. A. Kramers, Physica (Amsterdam) **7**, 284 (1940).
[25] S. El Amrani, F. Vigné, and B. Bigot, J. Phys. Chem. **96**, 9417 (1992).
[26] A. Miecznikowski and J. Hanuza, Zeolites **7**, 249 (1987).